





# Unexpected gene activation following CRISPR-Cas9-mediated genome editing

Anna G Manjón<sup>1,2,3</sup> , Simon Linder<sup>1,2,4</sup>, Hans Teunissen<sup>1,2,5</sup>, Anoek Friskes<sup>1,2,3</sup> , Wilbert Zwart<sup>1,2,4</sup>, Elzo de Wit<sup>1,2,5</sup>  & René H Medema<sup>1,2,3,\*</sup> 

## Abstract

The discovery of the Clustered Regularly Interspaced Short Palindromic Repeats (CRISPR) and its development as a genome editing tool has revolutionized the field of molecular biology. In the DNA damage field, CRISPR has brought an alternative to induce endogenous double-strand breaks (DSBs) at desired genomic locations and study the DNA damage response and its consequences. Many systems for sgRNA delivery have been reported in order to efficiently generate this DSB, including lentiviral vectors. However, some of the consequences of these systems are not yet well understood. Here, we report that lentiviral-based sgRNA vectors can integrate into the endogenous genomic target location, leading to undesired activation of the target gene. By generating a DSB in the regulatory region of the *ABCB1* gene using a lentiviral sgRNA vector, we can induce the formation of Taxol-resistant colonies. We show that these colonies upregulate *ABCB1* via integration of the *EEF1A1* and the U6 promoters from the sgRNA vector. We believe that this is an unreported CRISPR/Cas9 on-target effect that researchers need to be aware of when using lentiviral vectors for genome editing.

**Keywords** CRISPR-Cas9; drug resistance; gene activation; lentiviral integration; on-target effects

**Subject Categories** Chromatin, Transcription & Genomics; Methods & Resources

**DOI** 10.15252/embr.202153902 | Received 28 August 2021 | Revised 29 November 2021 | Accepted 30 November 2021 | Published online 20 December 2021

**EMBO Reports (2022) 23: e53902**

## Introduction

The discovery of the Clustered Regularly Interspaced Short Palindromic Repeats (CRISPR), their role in the prokaryotic immune system, and subsequent development as a genome editing tool has revolutionized the field of molecular biology (Mojica *et al*, 1993, 2005; van der Oost *et al*, 2009; Jinek *et al*, 2012; Cong *et al*, 2013;

Mali *et al*, 2013). In recent years, many laboratories have developed CRISPR/Cas9 as a tool that can be applied to study many different biological questions (Lino *et al*, 2018). In the DNA damage field, CRISPR has brought an alternative to induce endogenous double-strand breaks (DSBs) at desired genomic locations. This system allowed for the study of the DNA damage response and its consequences in different genome compartments or structures (Vitor *et al*, 2020). Combining imaging and high-throughput technologies with DSB-induced Cas9 systems allows one to examine processes such as transcription, chromatin dynamics, and DNA replication (Aymard *et al*, 2017; D'Alessandro & d'Adda di Fagagna, 2017; Clouaire & Legube, 2019; Miné-Hattab & Chiolo, 2020).

The CRISPR/Cas9 system needs to be delivered in an accurate manner for efficient gene editing.

On the one hand, the Cas9 protein needs to be expressed in the host system or delivered in the form of a ribonucleoprotein (RNP) complex (Jinek *et al*, 2014). On the other hand, a target-specific single-guide RNA (sgRNA)—formed by CRISPR RNA (crRNA) and transactivating CRISPR RNA—needs to direct Cas9 to the target site (Doudna & Charpentier, 2014). It is important to choose the right delivery strategy for the sgRNA to survive the degradation processes in the cell and translocate into the nucleus to allow for gene editing. To date, we can classify sgRNA delivery methods into viral and nonviral, based on whether viral constructs are used for transfection (Lino *et al*, 2018).

Viral vectors include gamma-retroviruses, adenovirus, adeno-associated viruses (AAVs), and lentiviruses (LVs) (Warnock *et al*, 2011). Especially in LVs, Cas9 and sgRNA are relatively easy to clone and produce to efficiently transduced into the host cell. HIV-1-based lentiviral vectors convert single-strand RNA into double-strand DNA by reverse transcription and subsequent insertion into the genome of postmitotic cells (Lino *et al*, 2018). Lentiviral vectors have become important tools to deliver components of the CRISPR/Cas9 system for genome editing. Yet, one of the bigger challenges of these systems is the random integration of the construct into the genome (Kotterman *et al*, 2015). In fact, in gene therapy, stable viral integrations come with concerns regarding safety (Rothe *et al*, 2014). Among them, the deregulation of genes caused by the

1 Oncode Institute, The Netherlands Cancer Institute, Amsterdam, The Netherlands

2 The Netherlands Cancer Institute, Amsterdam, The Netherlands

3 Division of Cell Biology, The Netherlands Cancer Institute, Amsterdam, The Netherlands

4 Division of Oncogenomics, The Netherlands Cancer Institute, Amsterdam, The Netherlands

5 Division of Gene Regulation, The Netherlands Cancer Institute, Amsterdam, The Netherlands

\*Corresponding author. Tel: +31 20 512 1990; E-mail: r.medema@nki.nl

insertions and mutagenesis was found in gene therapy for immunodeficiencies in patients (Hacein-Bey-Abina *et al*, 2003). The nonviral methods are divided into physical and chemical. Physical methods include microinjections—where the sgRNAs are directly injected by a needle—and electroporation—where electric currents open the cell membrane for the delivery of molecules into the cell (Horii *et al*, 2014; de Melo & Blackshaw, 2018). Chemical delivery methods comprise a DNA or RNA form of the sgRNA that can be used to transfect the host by liposome-based and non-leptosomic reagents (Felgner *et al*, 1987; Liang *et al*, 2015). With RNA delivery methods, the transfection efficiency can be lower, but they are a safer alternative, as random viral integrations do not occur.

Even though targeting genomic regions with the CRISPR/Cas9 system are tightly controlled and specific, it is known that off-target cutting activity can still occur (Cong *et al*, 2013; Hsu *et al*, 2013; Pattanayak *et al*, 2013). Other limitations of CRISPR include the requirement for a protospacer adjacent motif (PAM) to the target DNA sequence and the DNA-damage toxicity triggered through the CRISPR-induced DSB (Uddin *et al*, 2020). Nonetheless, valuable efforts have been made to understand and minimize these drawbacks. Many researchers are currently using lentiviral vectors for delivery of CRISPR/Cas9 components, as sgRNAs are relatively easy to clone into them (Lino *et al*, 2018). Lentiviral sgRNA-delivery systems are used in functional genetic screens to find lethal interactions of specific biological processes (Mulero-Sánchez *et al*, 2019). Even though many limitations are known regarding off-targets or difference in efficiency between sgRNAs (Zhang *et al*, 2015; Kosicki *et al*, 2018; Cao *et al*, 2020), much less is known about how viral CRISPR/Cas9 delivery methods may affect genome integrity and gene expression when randomly integrated into the host genome.

Here, we show that an LV-based sgRNA vector can integrate into the endogenous genomic target location, thereby affecting the expression of the target gene. By generating a DSB in the regulatory region of the *ABCB1* gene with this system, we can produce Taxol-resistant clones that upregulated *ABCB1* through transcriptional activation via the *EEF1A1* from the sgRNA vector. We speculate that targeted viral integration could result in deregulation of genes that may affect biological functions and therefore lead to false positive candidates, for instance, when performing functional genetic screens. Therefore, we believe that this unreported gene activation mechanism following CRISPR-Cas9-mediated genome editing needs to be taken into consideration when inducing DSBs with sgRNA lentiviral method.

## Results and Discussion

### A LentiGuide-induced DSB in the *ABCB1* promoter leads to upregulation of *ABCB1*

We have previously shown that in human retinal pigment epithelial-1 (RPE-1), a major mechanism of Taxol resistance is transcriptional activation of the *ABCB1* gene, that encodes for the multidrug resistance protein MDR1 or P-Glycoprotein (PgP) (Tame *et al*, 2017; preprint: Manjón *et al*, 2021). Using the lentiviral system LentiGuide-Puro from the Zhang Lab (Sanjana *et al*, 2014a), we cloned different sgRNAs targeting different noncoding regions across the *ABCB1* locus to induce a DSB (Fig 1A). We chose noncoding regions to avoid the possibility that a break-induced change in

coding sequence could result in acquired Taxol resistance. Seven days after lentiviral infection and puromycin selection, we treated the RPE-1 cells with 8 nM of Taxol in order to select cells that overexpressed PgP. Surprisingly, we observed that only cells treated with sgRNAs targeting the promoter of *ABCB1* became resistant to Taxol (Figs 1A and EV1A), as we observed a considerable number of RPE-1 colonies growing under Taxol pressure. Importantly, we also performed lentiviral infection with the same sgRNAs targeting *ABCB1* in human mammary epithelial cells (HMEC) expressing Cas9. Here, we also observed that the sgRNAs targeting the promoter of *ABCB1* lead to Taxol-resistant colonies (Fig EV1B).

In order to better understand the mechanisms responsible for the acquisition of the Taxol-resistant phenotype, we decided to individually characterize these Taxol-resistant clones that arose from sgRNA targeting of the *ABCB1* promoter. Therefore, we expanded the RPE-1-resistant colonies observed in the colony outgrowth assays in the presence of Taxol. When performing a viability assay with increasing doses of Taxol, we observed that all clones were resistant to high concentrations of Taxol, and could be resensitized with Tariquidar, a PgP inhibitor (Fig 1B). As expected, with Western Blot and qRT-PCR assays, we could confirm that the Taxol-resistant clones expressed high levels of PgP protein as well as mRNA, respectively (Fig 1C and D). Thus, confirming that the mechanism of Taxol resistance was through *ABCB1* upregulation. By performing intronic smRNA-FISH, which allows for visualization of active transcription sites, we demonstrated that only one allele was actively transcribing *ABCB1* (Fig 1E), confirming that *ABCB1* copy number amplifications were not observed in these clones. In order to assess whether a DSB in *ABCB1* was necessary to generate the Taxol-resistant colonies, we generated RPE-1 cells with a dCas9 construct. We then transduced the sgRNAs targeting *ABCB1* both in RPE-1 Cas9 and dCas9 cells followed by Puromycin and Taxol selection. Only cells with catalytically active Cas9 were able to generate Taxol-resistant colonies (Fig EV1C–E). All together, these results indicate that a subset of cells, which undergo Cas9-dependent DNA break formation in the *ABCB1* regulatory region, acquire Taxol resistance through *ABCB1* transcriptional activation.

### The LentiGuide vector integrates and drives gene expression upon a DSB in the *ABCB1* promoter

To exclude that DNA translocations or insertions might be induced by the DSB and could modify the activity of the *ABCB1* promoter, we performed Targeted Locus Amplification (TLA), a chromosome conformation capture-based technique, enabling the identification of single nucleotide variation and genomic rearrangements in a specific locus using a single PCR reaction (de Vree *et al*, 2014). We selectively amplified and sequenced the DNA flanking the *ABCB1* promoter. We compared RPE-1 parental cells with a Taxol-resistant clone derived from the sgRNA #6 targeting the promoter of *ABCB1* (sg6C9). Surprisingly, we found that our TLA experiments for the *ABCB1* promoter amplified a 1.3-kb region from chromosome 6 in the Taxol-resistant clone (Fig 2A, green arrow). When zooming in on that region, we discovered that the promoter of the *EEF1A1* gene was amplified in the sg6C9 Taxol-resistant clone (Fig 2B). The read distribution over the *EEF1A1* promoter is reminiscent of genomic insertions previously mapped with TLA (de Vree *et al*, 2014). To confirm the fusion of the *ABCB1* and *EEF1A1*, we performed PCRs



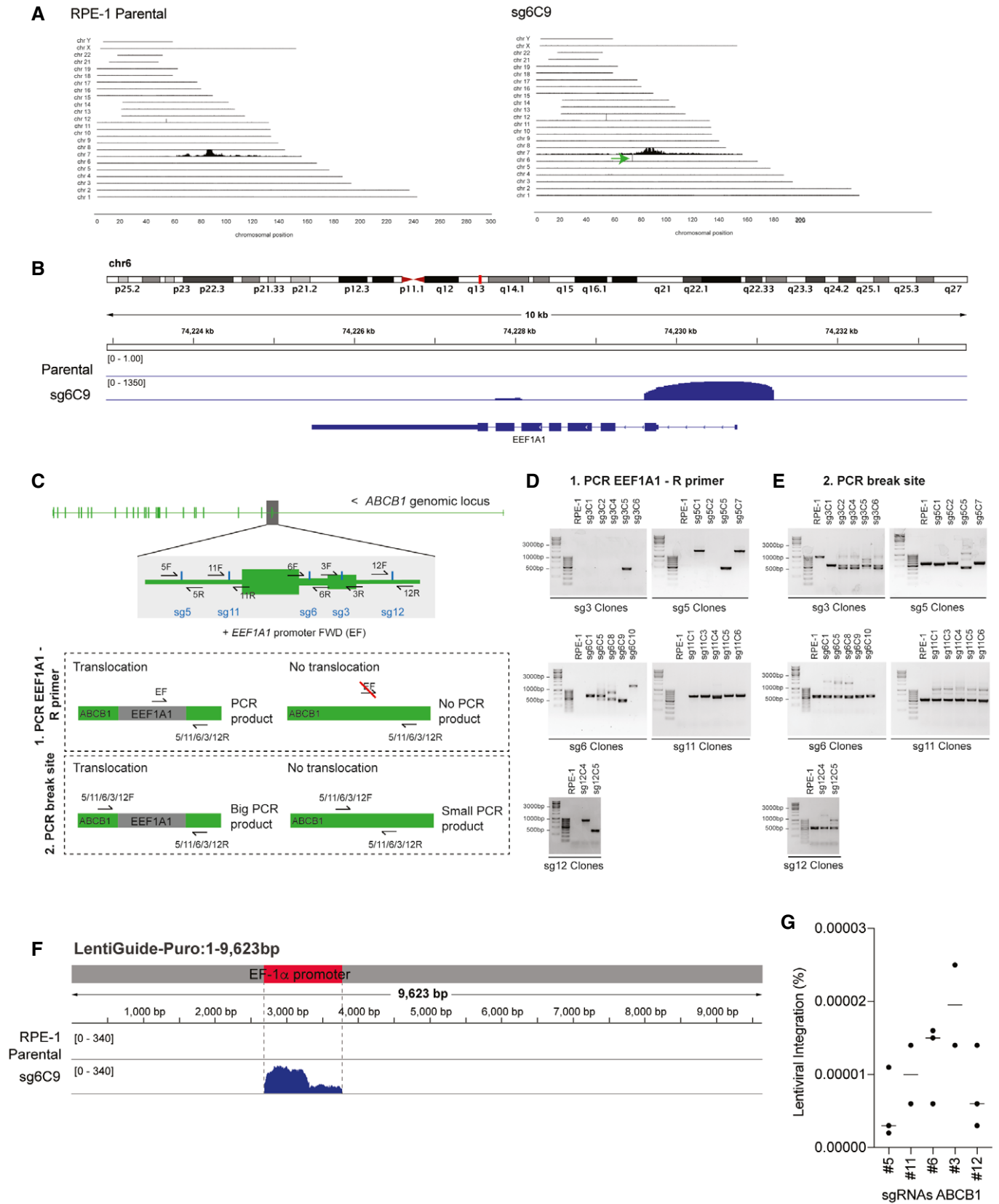


Figure 2.

**Figure 2. sgRNA integration and transcription activation of ABCB1.**

- A TLA analysis for *ABCB1* contacts in RPE-1 parental and Taxol-resistant clone sg6C9 covering the whole genome. Green arrow in sg6C9 shows a *de novo* interaction found between *ABCB1* and a region in chromosome 6.
- B TLA analysis for RPE-1 parental and sg6C9. Zoom in in the region of chr6 with *de novo* interaction for sg6C9. Image modified from IGV viewer.
- C Graphical representation of the PCR products to assess vector integration. Two different primer pairs were used to PCR the vector integration: (i) a common *EEF1A1* Forward (F) primer with a specific Reverse for each break site (5/11/6/3/12R). Only when *EEF1A1* is integrated in cis, we will obtain a PCR product. (ii) Forward and reverse primers are used to amplify each specific break site (5/11/6/3/12F and R). If *EEF1A1* is integrated in the break site, the PCR product will be bigger.
- D PCR products using the primers in C(1) over the *ABCB1* and *EEF1A1* regions in RPE-1 parental and the different Taxol-resistant clones.
- E PCR products using the primers in C(2) over the specific break site in the *ABCB1* promoter in RPE-1 parental and the different Taxol-resistant clones.
- F TLA analysis for RPE-1 parental and sg6C9. Reads are aligned to the lenti-guide vector. The location of the EF1 $\alpha$  promoter from the vector is highlighted in red. Image modified from IGV viewer.
- G Percentage of RPE-1 cells targeted with the *ABCB1* promoter sgRNAs found with vector integration. Percentages were calculated from data in Fig 1A. Each dot represents a CFA replicate experiment. Horizontal bars represent the mean of lentiviral integration per sgRNA.

the LentiGuide vector sequence that was used to clone the *ABCB1*-targeting sgRNAs to induce the DSB. We found that in the sg6C9 Taxol-resistant clone, there was a large region aligning with the LentiGuide vector belonging to the EF1 $\alpha$  promoter, suggesting that the *EEF1A1* integration found in the *ABCB1* promoter belonged to the LentiGuide vector and not to the endogenous gene found on chromosome 6 (Fig 2F).

We next decided to calculate the frequency of vector integration in the *ABCB1* locus following sgRNA-dependent DSB induction. Taxol-resistant clones with vector integration are highly resistant to Taxol (Figs 1B and EV2A) and were obtained from big colonies in the colony formation assays (Fig EV1A). Indeed, PCRs performed in smaller colonies derived from sgRNA #12 did not show evidence of LentiGuide integration (Fig EV2B). This correlates with the fact that they are more sensitive to Taxol and have lower mRNA levels of *ABCB1* (Fig EV2A and C). Therefore, in

order to estimate the frequency of vector integration, we decided to only count the big colonies from the colony formation assays. We could observe some variability on frequency depending on the sgRNA used (Fig 2G). We estimated that from Puromycin-selected cells, approximately 10 in a million cells will have the vector integrated in the DSB site (Fig 2G). This mechanism does not appear to be of high frequency, but the stringent selection system based on transcriptional activation of the *ABCB1* gene allows us to detect these infrequent events.

In order to know whether this phenomenon could be reproduced in other cell lines, we also performed PCRs over the DSB site in Taxol-resistant HMEC clones derived from the sgRNA #12 targeting the *ABCB1* promoter (Fig EV1B). Strikingly, in all the Taxol-resistant clones tested, we detected a higher PCR product than the expected one based on the endogenous *ABCB1* sequence (Fig EV3A). We therefore conclude that in both RPE-1 and HMEC

**Table 1. Blast search to find sequences producing significant alignments to PCR sequenced band of sg6C10 (EEF1A FWD + 6 REV). Top 10 sequences with best alignments found.**

Description	Scientific name	Max Score	Total Score	Query Cover	E value	Per. Identity	Acc. Len	Accession
Select seq MN996874.1	Cloning vector sh-AFP-PPP2CA, complete sequence	924	1318	56%	0.0	99.41%	8000	MN996874.1
Select seq MN996873.1	Cloning vector sh-PPP2CA.dna, complete sequence	924	1318	56%	0.0	99.41%	7716	MN996873.1
Select seq MN996872.1	Cloning vector sh-ctrl, complete sequence	924	1318	56%	0.0	99.41%	7717	MN996872.1
Select seq MN996871.1	Cloning vector sh-AFP, complete sequence	924	1318	56%	0.0	99.41%	7716	MN996871.1
Select seq KJ175229.1	Cloning vector pGL3-U6-sgRNA-PG, complete sequence	881	881	44%	0.0	94.62%	4952	KJ175229.1
Select seq MK801288.1	Cloning vector RS474_ErbB-RASER1C-dCas9VP64, complete sequence	680	1152	54%	0.0	95.00%	16350	MK801288.1
Select seq MH782475.1	Cloning vector pMJA289, complete sequence	680	1152	54%	0.0	95.21%	9466	MH782475.1
Select seq MH782474.1	Cloning vector pMJA284, complete sequence	680	1152	54%	0.0	95.21%	6739	MH782474.1
Select seq MH782473.1	Cloning vector pMJA285, complete sequence	680	1152	54%	0.0	95.21%	10035	MH782473.1
Select seq MG840314.1	Cloning vector pLenti-EF1a-dCas9-DNMT3B(E697A)-2A-bla, complete sequence	680	1152	54%	0.0	95.00%	14877	MG840314.1

cells, the LentiGuide-Puro vector had been integrated into the *ABCB1* promoter, most likely due to the presence of the CRISPR-induced DSB in that region. As the U6 promoter is an RNA Pol III promoter, most likely this will not result in mRNA and protein

translation. Therefore, most probably the *EEF1A1* promoter from this vector induced the transcriptional activation of *ABCB1*.

In order to understand whether LentiGuide vector integration was specific to the *ABCB1* gene, we set out to investigate whether

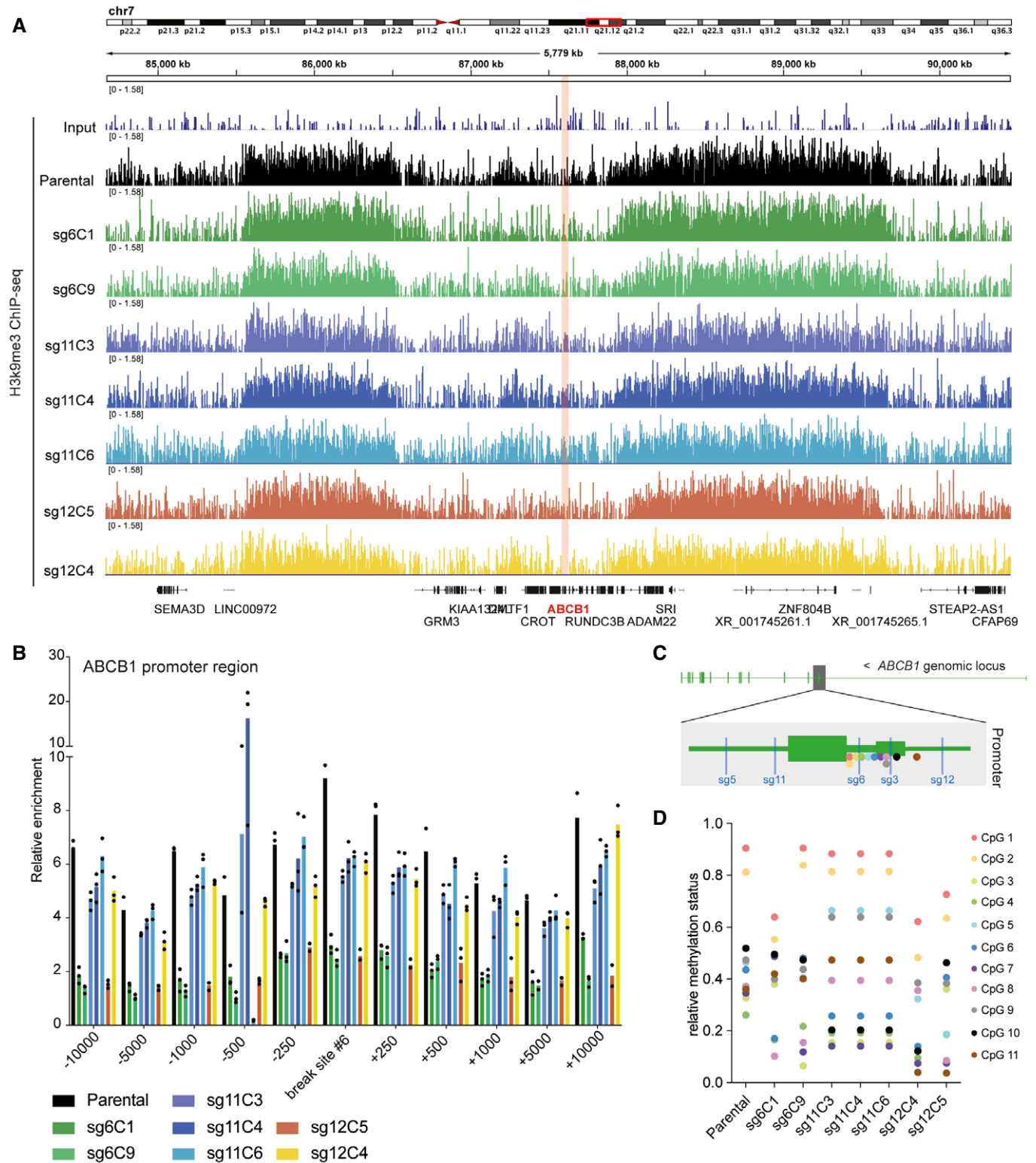




**Figure 3. Chromatin landscape in the *ABCB1* promoter region upon LentiGuide vector integration.**

- A H3K9me3 ChIP-sequencing tracks from the q21.12 arm of chromosome 7 in RPE-1 cells (parental and Taxol-resistant clones). The *ABCB1* gene region is shown in pink. Each colored track shows the H3K9me3 profile of a different Taxol-resistant clone.
- B H3K9me3 ChIP-qPCR in the *ABCB1* promoter region. Bar graph shows primer pairs amplifying the sgRNA#6 break and spanning this region (+/- base pairs) for each Taxol-resistant clone compared to the parental. Bar plots show the mean of H3K9me3 relative enrichment. Each dot represents a technical replicate ( $n = 3$ ).
- C Graphical representation of the *ABCB1* promoter region. The location of the sgRNAs targeting the promoter is shown in blue. The location of the eleven CpG islands analyzed in the methyl array are shown in colored dots.
- D Relative methylation status (1: methylated, 0: nonmethylated) of the eleven CpG islands shown in C for RPE-1 parental and the Taxol-resistant clones.

this phenomenon could happen in other genomic regions. Therefore, we generated an sgRNA targeting the regulatory region of *ABCG2*. *ABCG2* gene encodes for another drug efflux pump similar to *ABCB1*, which has been described to be responsible for Hoechst 33342 dye efflux (Scharenberg *et al*, 2002). Hoechst is a fluorescent compound, which can be incorporated by cells, which allows for fluorescence-activated cell sorting (FACS). We generated an RPE-1 cell line with overexpression of *ABCG2* (CRISPRa-*ABCG2*), which confirmed lower intracellular levels of Hoechst by FACS (Fig EV3B–D). We next induced a DSB in the promoter of *ABCG2* in RPE-1 Cas9 cells with a lentiviral system followed by Hoechst<sup>Low</sup> cell sorting (Fig EV3E). Strikingly, only the population targeted with the *ABCG2* sgRNA showed increased numbers of Hoechst<sup>Low</sup> cells. When performing PCRs over the DSB site in this polyclonal Hoechst<sup>Low</sup> population, we could observe higher DNA bands (Fig EV3F and G). Sanger sequence of the purified 750-bp band demonstrated that the *EEF1A1* promoter of the LentiGuide construct was integrated in the break site (Fig EV3H). Altogether, these data indicate that vector integration can also happen in other genic regions, which will lead to gene upregulation.

### Chromatin changes in the *ABCB1* promoter region upon LentiGuide vector integration

We next decided to compare the chromatin landscape of the *ABCB1* promoter in RPE-1 parental cells and the Taxol-resistant clones with the LentiGuide-Puro integration. It is known that in RPE-1 parental cells, *ABCB1* is found in a repressive chromatin environment, consequently leading to transcriptional repression (preprint: Manjón *et al*, 2021). We therefore performed chromatin immunoprecipitation followed by massive parallel sequencing (ChIP-seq) for the repressive histone modification H3K9me3. ChIP-sequencing tracks of this chromatin mark showed that in RPE-1 parental cells, *ABCB1* is located in a region that contains intermediate level of H3K9me3, flanked by regions with high levels of H3K9me3 (Fig 3A, black track). Importantly, the seven Taxol-resistant clones derived from different sgRNAs also displayed a similar H3K9me3 pattern (Fig 3A). In order to better quantify the levels of H3K9me3, we performed ChIP-qPCRs of the *ABCB1* promoter spanning up to 10 kb surrounding the transcriptional start site (Fig 3B). Interestingly, we observed that while some Taxol-resistant clones had lower levels of H3K9me3 (sg6C1, sg6C9, and sg12C5), others had similar levels compared to the parental cell line (sg11C3-4-6 and sg12C4) (Figs 3B and EV4A). It has been suggested that DNA methylation of the *ABCB1* promoter can regulate its transcriptional status (Chen *et al*, 2005; Reed *et al*, 2010). Therefore, we set out to study whether the DNA methylation pattern was altered in the Taxol-resistant clones. By performing a DNA methylation array, we could assess the relative methylation status of 11 CpG

islands located in close proximity to the sgRNAs targeting regions within the *ABCB1* promoter (Fig 3C and D). In parental RPE-1 cells, only two CpG islands were nearly fully methylated (CpG 1 and 2) and maintained the same status in four out of seven Taxol-resistant clones (Fig 3D). The remaining CpG islands were hemi-methylated in the parental cell line and vary between clones (Fig 3D). Therefore, even though some Taxol-resistant clones showed lower levels of repressive chromatin marks as compared to their parental Taxol-sensitive counterpart, others that maintained these levels still resulted in *ABCB1* gene activation. Possibly, the DNA damage-repair process induced by the sgRNA-Cas9 system could cause the erasure of repressive chromatin marks, but this does not fully explain the observed *ABCB1* gene activation pattern. Therefore, we suggest that the endogenous *ABCB1* promoter remains repressed in (at least a subset of) the Taxol-resistant clones containing the LentiGuide-Puro integration, and that transcriptional activation occurs via the *EEF1A1* promoter present in that vector.

Altogether, in this study, we show that a lentiviral sgRNA delivery system used to induce a DSB close to the transcriptional start site of a gene can result in the integration of the vector in the break site and subsequent activation of the gene. When generating a DSB in the regulatory region of *ABCB1* with this system, we were able to find cells with genetic alterations that contained the U6 and *EEF1A1* promoters of the lentiviral vector. We believe that the DSB increased the probability of the vector to integrate into this location. In RPE-1 cells, *ABCB1* is repressed and the cells are sensitive to Taxol. The integration of these promoters allowed for gene activation and produced a Taxol-resistant phenotype (Fig 4). Furthermore, as CRISPR enables the induction of DNA breaks at specific endogenous loci, more and more researchers are using several Cas9 systems to study of DSB repair and its biological consequences (Vítor *et al*, 2020; Van Den Berg *et al*, 2018; Schep *et al*, 2021). As we show here, inducing a DSB in a gene regulatory region can have consequences in gene expression, thus leading to incorrect interpretation of the results. Therefore, to study long-term consequences of the DNA damage response, we suggest to employ nonintegrative systems such as synthetic gRNAs delivered in the form of RNA complexes (Yan & Schubert, 2017).

## Materials and Methods

### Cell lines and cell culture conditions

RPE-1 cells are hTert-immortalized human retinal pigment epithelium nontumoral cells. HMEC cells are hTert-immortalized human mammary epithelial nontumoral cells. RPE-1 and HMEC Cas9 cells were generated

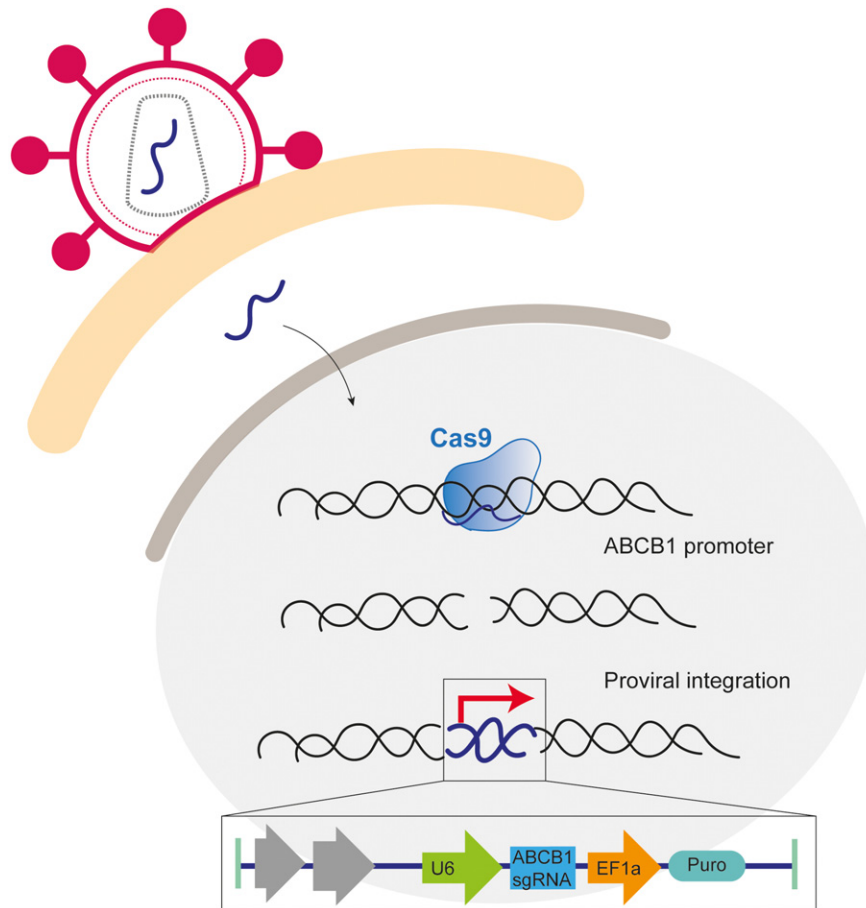


**Figure 4. Model of sgRNA integration in endogenous *ABCB1* locus.**

When a lenti-guide Puro vector is used to deliver a gRNA to induce a DSB, the gRNA can be integrated into the break site. The DSB was induced in the promoter of *ABCB1* and therefore the highly active promoters of the vector were driving the expression of the *ABCB1* gene. In this case, we were selecting for cells that upregulated *ABCB1* and therefore the frequency of this event was higher.

by lentiviral transduction with a lenti-Cas9-Blast (Addgene #73310) and Blasticidine S selection with 10 µg/ml. RPE-1 dCas9 cells were generated by cotransduction with the viral particles containing SunTag-dCas9-BFP (Addgene #60910) and selected on BFP positivity. RPE-1 and HMEC cell lines were maintained in DMEM/F-12 + Glutamax (Gibco, Life Technology) supplemented with 1% penicillin/streptomycin and 6% fetal bovine serum (FBS, S-FBS-EU-015, Serana).

### Compound treatments

Taxol and Tariquidar were dissolved in DMSO and prepared at stock concentrations before usage at varying final concentrations as indicated in each figure. Hoechst 33342 was used at a final concentration of 0.1 µg/ml.

### sgRNA designed and cloning

The sgRNAs targeting *ABCB1* were cloned into a LentiGuide-Puro (Addgene plasmid # 52963) using the BsmBI restriction site following the original protocol (Sanjana *et al.*, 2014b; Shalem *et al.*, 2014). sgRNA sequences are summarized in Table 2.

### HEK cells transfection and virus production

In order to generate the lentiviral sgRNAs, two million HEK 293T cells were plated followed by DNA transfection. In 200 µl of Opti-MEM™ (Reduced Serum Medium), 2 µg of psPAX and 2 µg of pMD2G packaging plasmids were cotransfected with 2 µg of the corresponding sgRNA vector. Sixteen microliters of FuGENE® 6 were used as lipid-based transfection reagent. Twenty-four-hour posttransfection, the medium was exchanged and for 24 h, the virus was collected for further experiments.

### sgRNA lentiviral infection and colony formation assays

Of 400,000 RPE-1 or HMEC cells were infected with a specific lenti-sgRNA in 1:4 ratio. Next day, cells were trypsinized and 10 µg/ml of Puromycin was added. Cells were allowed to grow under Puromycin selection for 7 days. Following selection, 1 million cells were seeded and treated with 8 nM of Taxol and allowed to grow out for 15 days. Plates were fixed in 80% methanol and stained with 0.2% Crystal Violet solution. After fixation, the number of Taxol-resistant cells was counted.



## Viability assays

For viability assays, 1,000 cells were plated in a 96-well plate and treated for 7 days with indicated drug concentrations. Subsequently, plates were fixed in 80% methanol and stained with 0.2% Crystal Violet solution.

## RNA isolation and qRT-PCR analysis

RNA isolation was performed by using Qiagen RNeasy kit and quantified using NanoDrop (Thermo Fisher Scientific). cDNA was synthesized using Bioscript reverse transcriptase (Bioline), Random Primers (Thermo Fisher), and 1,000 ng of total RNA according to the manufacturer's protocol. Primers were designed with a melting temperature close to 60 degrees to generate 90–120-bp amplicons, mostly spanning introns. cDNA was amplified for 40 cycles on a cycler (model CFX96; Bio-Rad Laboratories) using SYBR Green PCR Master Mix (Applied Biosystems). Target cDNA levels were analyzed by the comparative cycle (Ct) method and values were normalized against GAPDH expression levels. qRT-PCR oligo sequences are summarized in Table 3.

## Western Blots

For western blot experiments, equal amounts of cells were lysed with Laemmli buffer and separated by SDS–polyacrylamide gel

electrophoresis followed by transfer to a nitrocellulose membrane. Membranes were blocked in 5% milk in PBST for 1 h at RT before overnight incubation with primary antibody in PBST with 5% milk at 4°C. Membranes were washed three times with PBST followed by incubation with secondary antibody in PBST with 5% milk for 2 h at RT. Antibodies were visualized using enhanced chemiluminescence (ECL) (GE Healthcare). The following antibodies were used for western blot experiments:  $\alpha$ -Tubulin (Sigma t5168), MDR(PgP) (sc-8313). For secondary antibodies, peroxidase-conjugated goat anti-rabbit (P448 DAKO, 1:2,000), goat anti-mouse (P447 DAKO, 1:2,000), and rabbit anti-goat (P449) were used.

## smRNA FISH

RPE-1 cells were plated on glass coverslips and washed twice with BS before fixation in 4% PFA in PBS for 10 min at room temperature. After two additional washes in 1× PBS, coverslips were incubated in 70% ethanol at 4°C overnight. Coverslips were incubated for prehybridization in wash buffer (2× saline-sodium citrate (SSC) with deionized formamide (Sigma) 10%) for 2–5 min at room temperature. RNA FISH probe mix wash was dissolved in hybridization buffer (wash buffer supplemented with 10% dextran sulfate). Thirty-eight probes labeled with Cy5 were targeted to the intronic regions of *ABCB1* (Biosearch Technologies). Coverslips were incubated in hybridization solution for at least 4 h at 37°C. Then coverslips were washed twice for 30 min with wash buffer followed by a quick rinse with 2× SSC. Finally, coverslips were washed once for 5 min in 1× PBS before mounting on slides using Prolong gold DAPI mounting medium (Life Technologies). Images were acquired with the use of a DeltaVision Elite (Applied Precision) equipped with a 60× 1.45 numerical aperture (NA) lens (Olympus) and cooled CoolSnap CCD camera. *ABCB1* transcription start site quantification was performed manually double blind.

## TLA analysis

TLA was performed as previously described with minor modifications. TLA libraries were sequenced on an MiSeq and were mapped to genome using bwa bwsw (Li & Durbin, 2010) to enable partial mapping of sequence reads. Reads were mapped to hg19 reference of the human genome.

## PCR to assess vector integration

500,000 RPE-1 or HMEC cells were lysed using DirectPCR Cell (Viagen). Two hundred milliliters  $\mu$ l of reagent and ~20  $\mu$ l of proteinase K (20 mg/ml) were added to each sample. Samples were incubated at 55°C for 4–6 h, followed by 85°C for 45 min to inactivate the proteinase K. Phusion polymerase was used for DNA amplification in the following protocol: 4  $\mu$ l 5× HF, 0.4  $\mu$ l dNTPs, 1  $\mu$ l of FWD

**Table 2. gRNA sequences targeting ABCB1.**

Name	Target gene	gRNA sequence
LentiGuide-Puro-ABCB1 #1	ABCB1	GCTGCTTTAAAAGGTCGCGG
LentiGuide-Puro-ABCB1 #2	ABCB1	AGAAAGCTCCATCAACCGCA
LentiGuide-Puro-ABCB1 #3	ABCB1	GCTGGGCAGAACAGCGCCG
LentiGuide-Puro-ABCB1 #4	ABCB1	TGTGACTGCTGATCACCAGCA
LentiGuide-Puro-ABCB1 #5	ABCB1	GCTTTCCTGCCCCAGACAGG
LentiGuide-Puro-ABCB1 #6	ABCB1	CCTCCCGTTCCAGTCGCGG
LentiGuide-Puro-ABCB1 #7	ABCB1	CTGCTCCTCCAATGAAAGG
LentiGuide-Puro-ABCB1 #8	ABCB1	GGTTTCCCCTGTAATAGA
LentiGuide-Puro-ABCB1 #9	ABCB1	CCTATTGCTCTGATGGCG
LentiGuide-Puro-ABCB1 #10	ABCB1	ATACAATCCAAGAAAAACAA
LentiGuide-Puro-ABCB1 #11	ABCB1	ACAAACTTCTGCTCTAAGCA
LentiGuide-Puro-ABCB1 #12	ABCB1	TCAATGCCCGTGTITTTCCA
LentiGuide-Puro-ABCB1 #13	ABCB1	ATATTATCCCTGTTAATGCA
LentiGuide-Puro-ABCB1 #14	ABCB1	CCAAGAAGAAATGAAGCCAGA
LentiGuide-Puro-ABCB1 #15	ABCB1	CTAAGCCATGTAACCTTTCCG
LentiGuide-Puro-ABCG2 #5	ABCG2	GCGATAAGCGCCCTGCGACC

**Table 3. RT-qPCR primers.**

RT-qPCR primers	FWD	REV
ABCB1	ACAGCACGGAAGGCCTAATG	GTCTGGCCCTTCTTCACTC
GAPDH	TGCACCACCAACTGCTTA	GGATGCAGGGATGATGTTT
ABCG2	TTTCCAAGCGTTCATTCAAAA	TACGACTGTGACAATGATCTGACC

**Table 4. PCR primers to assess vector integration.**

Break site primers	FWD	REV
sgRNA ABCB1 #3	CTTCTCCCCTGAAGACCAAG	TAAATGCGAATCCCGAGAAA
sgRNA ABCB1 #5	GCAGAGCACCATGATCAAAA	caagtcgggtattgaagg
sgRNA ABCB1 #6	CTTCTTTGCTCTCCATTGC	GCTTCTTGAGGCGTGATAG
sgRNA ABCB1 #12	GGGAAATTTTCTCGGGATTC	AAGCTCTGATGTGAGTTAGCATTG
sgRNA ABCG2 #5	taacttgctctgggtgcgag	gtttccccagggtcggggttc
EEF1A1 FWD	CACGGCGACTACTGCACTTA	

**Table 5. ChIP-qPCR primers.**

	FWD	REV
ChIP-qPCR controls		
7 (negative control)	TGCCACACACCAGTGACTTT	ACAGCCAGAAGCTCCAAAAA
S2 (negative control)	CTAGGAGGGTGGAGGTAGGG	GCCCCAAACAGGAGTAATGA
KS6 (positive control)	TGAAGACACATCTGCGAACC	TCGCGCACTCATAAGTTTC
KS7 (positive control)	CAATTGGCCATATCTTTACG	CATGTTCTCGAAAGCAAGCA
ChIP-qPCR ABCB1		
250–	CCATTCCGACCTGAAGAGAAA	CTATTACTGCTCTCTGGCTTC
500–	TTCTGCTCTAAGCAGGGATATTG	CTAGCCTCCAGCTCTGAAATAAA
1,000–	GGCGACCAACACCACTT	GTCTTGGTGTGCTCTTTCT
5,000–	AGAGGTGCTTGATGTAATG	GCCACCATTCTGACTTAGAT
10,000–	CAGGGTACCTGGTTAGATTG	GGATGAAGTATCCTCTCTGTC
250+	GAAGAGCCGCTACTCGAATG	ATCTGTGGTGAGGCTGATTG
500+	CTACAGGACGTAGTTAAGGAAAT	AGGAGGCAGAAAGGTGATACAG
1,000+	TTCTGTCCACTATTTACTTCAAAC	GCTCTGATGTGAGTTAGCATTG
5,000+	GACTTACTAGCTGTGTGGCTTT	GAGCAGTGGAGTATTTCTTCAAATG
10,000+	GGCAAAGGCAACCTTCTTAC	CACCCAAGTGGCAATTTCTG

**Table 6. sgRNAs for CRISPRa ABCG2 upregulation with overhangs for BsmBI cloning.**

RT-qPCR controls	FWD	REV
ABCG2 CRISPRa #1	CACCGGTACCACCGCCCTCCCTCG	AAACCGAGGGAGGGCGGTGGTACC
ABCG2 CRISPRa #2	CACCGGCCGGAGCGCCAAGCACC	AAACGGTGCTTCGGCGCTCCGGCC
ABCG2 CRISPRa #3	CACCGGGGAGACCCGGACATCCAG	AAACCTGGATGTCGGGTCTCCCC
ABCG2 CRISPRa #4	CACCGACATCCAGGGACGAGCTC	AAACGAGCTCGTCCCTGGATGTC
ABCG2 CRISPRa #5	CACCGAAACCCGGGGCGCTGGGA	AAACTCCCCAGCGCCCCGGTTTC

primer, 1 µl of REV primer, 1 µl of DNA, 0.2 µl of Phusion polymerase and 12.4 µl of H<sub>2</sub>O. PCR cycles (×30): 98°C 30" - 98°C 10" - 58°C 30" - 72°C 2' - 72°C 10'. DNA samples were loaded in a 1.5% agarose gel and visualized using UV light (BioRad). Primers used for PCR can be found in Table 4.

#### ChIP-seq and ChIP-qRT-PCR of RPE-1 hTERT cells

Chromatin immunoprecipitations (ChIP) were performed as described previously (Prekovic *et al.*, 2021) with minor adjustments. Approximately  $7 \times 10^6$  cells per condition were fixed, 50 µl of

Protein A magnetic beads (Invitrogen) and 5 µg of antibody H3K9me3 (abcam ab8898). For ChIP-seq, samples were processed for library preparation (Part# 0801-0303, KAPA Biosystems kit), sequenced using an Illumina HiSeq2500 genome analyzer (65 bp reads, single end), and aligned to the Human Reference Genome (hg19) using Burrows-Wheeler Aligner (bwa) version 0.5.9. Mapped reads were filtered based on mapping quality of 20 using samtools version 0.1.19. For ChIP-qPCR analysis, DNA was amplified for 40 cycles on a cycler (model CFX96; Bio-Rad Laboratories) using SYBR Green PCR Master Mix (Applied Biosystems). Target DNA levels were analyzed by the comparative cycle (Ct) method and values

were normalized against input DNA and positive control region (specific for each chromatin mark). ChIP-qPCR oligo locations are summarized in Table 5.

### Generation of dCas9 and CRISPRa cell lines

For dCas9 experiments, RPE cells were transduced with viral particles containing SunTag-dCas9-BFP (Addgene# 60910). After 1 week of culturing, fluorescence-activated cell sorting (FACS) was used to select for cells that were BFP positive. Polyclonal CRISPRa cell lines were obtained, which were subsequently transduced with viral particles containing sgRNAs targeting *ABCB1* (#4, #7, #6 and #12). For CRISPRa experiments, a previously generated RPE-1 cell line containing SunTag-dCas9-BFP (Addgene# 60910) and scFV-VP69-GFP (Addgene# 60904) was used (Tame *et al*, 2017). The indicated cell line was transduced with viral particles containing pools of sgRNAs targeted at the promoter of *ABCG2*. Cells were selected for 2 weeks with puromycin to obtain stable polyclonal cell lines for the sgRNA expression. The sgRNAs used can be found in Table 6.

### DNA methylation array

DNA methylation was measured with the Infinium MethylationEPIC BeadChip (Illumina Inc., San Diego, CA) according to the manufacturer's protocol. In short, 500 ng of genomic DNA was bisulfite converted using the EZ-96 DNA Methylation Deep-Well Kit (Zymo Research, Irvine, CA, USA). The samples were plated in a randomized order. The bisulfite conversion was performed according to the manufacturers' protocol with the following modifications. For binding of the DNA, 15  $\mu$ l of MagBinding Beads was used. The conversion reagent incubation was done according to the following cycle protocol: 16 cycles of 95°C for 30 s followed by 50°C for 1 h. After the cycle protocol, the DNA is incubated for 10 min at 4°C. Next, DNA samples were hybridized on the Infinium MethylationEPIC BeadChip (Illumina Inc., San Diego, CA) according to the manufacturer's protocol.

## Data availability

All sequencing raw and processed data files generated in this study are available in GEO with the GEO accession code GSE185725 (<https://www.ncbi.nlm.nih.gov/geo/query/acc.cgi?acc=GSE185725>).

**Expanded View** for this article is available online.

### Acknowledgements

This work was supported by ZonMW-TOP grant 91215067 (RHM, AGM, and AF). EdW and HT are supported by an ERC StG (HAP-PHEN 637587). EdW is also supported by an ERC CoG FuncDis3D 865459. The Oncode Institute is partly supported by KWF Dutch Cancer Society.

### Author contributions

Conceived and designed study: AGM, RHM. Experiments: AGM, SL, HT, AF, WZ. Data processing, bioinformatics: EdW. Discussion and interpretation of data: AGM, RHM. Manuscript writing: AGM, RHM, with input from all authors.

### Conflict of interest

Elzo de Wit is cofounder of Cergentis B.V. which commercializes the TLA technology.

## References

- Aymard F, Aguirrebengoa M, Guillou E, Javierre BM, Bugler B, Arnould C, Rocher V, Iacovoni JS, Biernacka A, Skrzypczak M *et al* (2017) Genome-wide mapping of long-range contacts unveils clustering of DNA double-strand breaks at damaged active genes. *Nat Struct Mol Biol* 24: 353–361
- Cao JX, Wang YL, Wang ZX (2020) Advances in precise regulation of CRISPR/Cas9 gene editing technology. *Yi Chuan = Hered* 42: 1168–1177
- Chen KG, Wang YC, Schaner ME, Francisco B, Durán GE, Juric D, Huff LM, Padilla-Nash H, Ried T, Fojo T *et al* (2005) Genetic and epigenetic modeling of the origins of multidrug-resistant cells in a human sarcoma cell line. *Cancer Res* 65: 9388–9397
- Clouaire T, Legube G (2019) A snapshot on the cis chromatin response to DNA double-strand breaks. *Trends Genet* 35: 330–345
- Cong L, Ran FA, Cox D, Lin S, Barretto R, Habib N, Hsu PD, Wu X, Jiang W, Marraffini LA *et al* (2013) Multiplex genome engineering using CRISPR/Cas systems. *Science* 339: 819–823
- D'Alessandro G, d'Adda di Fagnagna F (2017) Transcription and DNA damage: holding hands or crossing swords? *J Mol Biol* 429: 3215–3229
- de Vree PJP, de Wit E, Yilmaz M, van de Heijning M, Klous P, Versteegen MJAM, Wan YI, Teunissen H, Krijger PHL, Geeven G *et al* (2014) Targeted sequencing by proximity ligation for comprehensive variant detection and local haplotyping. *Nat Biotechnol* 32: 1019–1025
- Doudna JA, Charpentier E (2014) The new frontier of genome engineering with CRISPR-Cas9. *Science* 346: 1258096
- Felgner P, Gadek T, Holm M, Roman R, Chan H, Wenz M, Northrop J, Ringold G, Danielsen M (1987) Lipofection: a highly efficient, lipid-mediated DNA-transfection procedure. *Proc Natl Acad Sci USA* 84: 7413–7417
- Hacein-Bey-Abina S, von Kalle C, Schmidt M, Le Deist F, Wulffraat N, McIntyre E, Radford I, Villeval J-L, Fraser CC, Cavazzana-Calvo M *et al* (2003) A serious adverse event after successful gene therapy for X-linked severe combined immunodeficiency. *N Engl J Med* 348: 255–256
- Horii T, Arai Y, Yamazaki M, Morita S, Kimura M, Itoh M, Abe Y, Hatada I (2014) Validation of microinjection methods for generating knockout mice by CRISPR/Cas-mediated genome engineering. *Sci Rep* 4: 4513
- Hsu PD, Scott DA, Weinstein JA, Ran FA, Konermann S, Agarwala V, Li Y, Fine EJ, Wu X, Shalem O *et al* (2013) DNA targeting specificity of RNA-guided Cas9 nucleases. *Nat Biotechnol* 31: 827–832
- Jinek M, Chylinski K, Fonfara I, Hauer M, Doudna JA, Charpentier E (2012) A programmable dual-RNA-guided DNA endonuclease in adaptive bacterial immunity. *Science* 337: 816–821
- Jinek M, Jiang F, Taylor DW, Sternberg SH, Kaya E, Ma E, Anders C, Hauer M, Zhou K, Lin S *et al* (2014) Structures of Cas9 endonucleases reveal RNA-mediated conformational activation. *Science* 343: 1247997
- Kosicki M, Tomberg K, Bradley A (2018) Repair of double-strand breaks induced by CRISPR-Cas9 leads to large deletions and complex rearrangements. *Nat Biotechnol* 36: 765–771
- Kotterman MA, Chalberg TW, Schaffer DV (2015) Viral vectors for gene therapy: translational and clinical outlook. *Annu Rev Biomed Eng* 17: 63–89
- Li H, Durbin R (2010) Fast and accurate long-read alignment with Burrows-Wheeler transform. *Bioinformatics* 26: 589–595
- Liang X, Potter J, Kumar S, Zou Y, Quintanilla R, Sridharan M, Carte J, Chen W, Roark N, Ranganathan S *et al* (2015) Rapid and highly efficient

- mammalian cell engineering via Cas9 protein transfection. *J Biotechnol* 208: 44–53
- Lino CA, Harper JC, Carney JP, Timlin JA (2018) Delivering crispr: a review of the challenges and approaches. *Drug Deliv* 25: 1234–1257
- Mali P, Yang L, Esvelt KM, Aach J, Guell M, DiCarlo JE, Norville JE, Church GM (2013) RNA-guided human genome engineering via Cas9. *Science* 339: 823–826
- Manjón AG, Hupkes DP, Liu NQ, Friskes A, Joosten S, Teunissen H, Aarts M, Prekovic S, Zwart W, De Wit E et al (2021) Perturbations in 3D genome organization can promote acquired drug resistance. *bioRxiv* <https://doi.org/10.1101/2021.02.02.429315> [PREPRINT]
- de Melo J, Blackshaw S (2018) In vivo electroporation of developing mouse retina. *Methods Mol Biol* 1715: 101–111
- Miné-Hattab J, Chiolo I (2020) Complex chromatin motions for DNA repair. *Front Genet* 11: 800
- Mojica FJM, Díez-Villaseñor C, García-Martínez J, Soria E (2005) Intervening sequences of regularly spaced prokaryotic repeats derive from foreign genetic elements. *J Mol Evol* 60: 174–182
- Mojica FJM, Juez G, Rodríguez-Valera F (1993) Transcription at different salinities of *Haloferax mediterranei* sequences adjacent to partially modified PstI sites. *Mol Microbiol* 9: 613–621
- Mulero-Sánchez A, Pogacar Z, Vecchione L (2019) Importance of genetic screens in precision oncology. *ESMO Open* 4: e000505
- van der Oost J, Jore MM, Westra ER, Lundgren M, Brouns SJJ (2009) CRISPR-based adaptive and heritable immunity in prokaryotes. *Trends Biochem Sci* 34: 401–407
- Pattanayak V, Lin S, Guilinger JP, Ma E, Doudna JA, Liu DR (2013) High-throughput profiling of off-target DNA cleavage reveals RNA-programmed Cas9 nuclease specificity. *Nat Biotechnol* 31: 839–843
- Prekovic S, Schuurman K, Mayayo-Peralta I, Manjón AG, Buijs M, Yavuz S, Wellenstein MD, Barrera A, Monkhorst K, Huber A et al (2021) (2021) Glucocorticoid receptor triggers a reversible drug-tolerant dormancy state with acquired therapeutic vulnerabilities in lung cancer. *Nat Commun* 12: 1–18
- Reed K, Hembruff SL, Sprowl JA, Parissenti AM (2010) The temporal relationship between ABCB1 promoter hypomethylation, ABCB1 expression and acquisition of drug resistance. *Pharmacogenomics J* 10: 489–504
- Rothe M, Modlich U, Schambach A (2014) Biosafety challenges for use of lentiviral vectors in gene therapy. *Curr Gene Ther* 13: 453–468
- Sanjana NE, Shalem O, Zhang F (2014a) Improved vectors and genome-wide libraries for CRISPR screening. *Nat Methods* 11: 783
- Sanjana NE, Shalem O, Zhang F (2014b) Improved vectors and genome-wide libraries for CRISPR screening. *Nat Methods* 11: 783–784
- Scharenberg CW, Harkey MA, Torok-Storb B (2002) The ABCG2 transporter is an efficient Hoechst 33342 efflux pump and is preferentially expressed by immature human hematopoietic progenitors. *Blood* 99: 507–512
- Schep R, Brinkman EK, Leemans C, Beijersbergen RL, Medema RH, Van B, Correspondence S (2021) Impact of chromatin context on Cas9-induced DNA double-strand break repair pathway balance
- Shalem O, Sanjana NE, Hartenian E, Shi Xi, Scott DA, Mikkelsen TS, Heckl D, Ebert BL, Root DE, Doench JG et al (2014) Genome-scale CRISPR-Cas9 knockout screening in human cells. *Science* 343: 84–87
- Tame MA, Manjón AG, Belokhvostova D, Raaijmakers JA, Medema RH (2017) TUBB3 overexpression has a negligible effect on the sensitivity to taxol in cultured cell lines. *Oncotarget* 8: 71536
- Uddin F, Rudin CM, Sen T (2020) CRISPR gene therapy: applications, limitations, and implications for the future. *Front Oncol* 10: 1387
- Van Den Berg J, Manjón AG, Manjón M, Kielbassa K, Feringa FM, Freire R, Medema RH (2018) A limited number of double-strand DNA breaks is sufficient to delay cell cycle progression. *Nucleic Acids Res* 46: 10132–10144
- Vítor AC, Huertas P, Legube G, de Almeida SF (2020) Studying DNA double-strand break repair: an ever-growing toolbox. *Front Mol Biosci* 7: 24
- Warnock JN, Daigre C, Al-Rubeai M (2011) Introduction to viral vectors. *Methods Mol Biol* 737: 1–25
- Yan S, Schubert M, Young M, Wang B (2017) Applications of Cas9 nickases for genome engineering
- Zhang XH, Tee LY, Wang XG, Huang QS, Yang SH (2015) Off-target effects in CRISPR/Cas9-mediated genome engineering. *Mol Ther - Nucleic Acids* 4: e264



**License:** This is an open access article under the terms of the Creative Commons Attribution-NonCommercial-NoDerivs License, which permits use and distribution in any medium, provided the original work is properly cited, the use is non-commercial and no modifications or adaptations are made.